ESCAP/WMO
Typhoon Committee

Available online at www.sciencedirect.com

ScienceDirect

Tropical Cyclone Research and Review 12 (2023) 123–135

www.keaipublishing.com/tcrr

Forecasting tropical cyclone tornadoes and impacts: Report from IWTC-X

Dereka Carroll-Smith [a,b], Benjamin W. Green [c,d,*], Roger Edwards [e], Lanqiang Bai [f], A.J. Litta [g], Xianxiang Huang [f], Lauren Pattie [h], Scott Overpeck [i], Eugene W. McCaul Jr. [j]

[a] *University of Maryland, College Park, MD, USA*
[b] *Jackson State University, Jackson, USA*
[c] *Cooperative Institute for Research in Environmental Sciences, University of Colorado, Boulder, USA*
[d] *NOAA Global Systems Laboratory, Boulder, USA*
[e] *NOAA/NWS/Storm Prediction Center, Norman, USA*
[f] *Foshan Tornado Research Center, China Meteorological Administration Tornado Key Laboratory, Guangzhou, China*
[g] *Weathernews Inc., Chiba, Japan*
[h] *Environmental Prediction Services, Australian Bureau of Meteorology, Brisbane, Australia*
[i] *NOAA/NWS/Weather Forecast Office, Albuquerque, USA*
[j] *Science and Technology Institute, Universities Space Research Association, Huntsville, USA*

Available online 3 June 2023

Abstract

This report synthesizes global tropical cyclone (TC) tornado research and operational practices to date. Tornadoes are one of the secondary (and lesser researched) hazards contributing to the devastation TCs leave in their wake. While gale-force winds and storm surge produce the majority of damage and fatalities globally, TC tornadoes also pose a fatal threat, complicating evacuation plans and protective actions as the storm moves inland. Climatological studies characterize TC-spawned tornadoes as usually weak and short-lived, primarily originating from miniature supercells in the outer rainbands. These tornadic features pose challenges to forecasting and radar detection. Additionally, TC tornadoes can pose a threat to communities 12 h prior to and beyond 48 h after a TC makes landfall.

Research, both basic and operational, has increased globally over the last few years in efforts to move from a climatological to ingredients-based approach to detect and forecast TC tornadoes. While the United States has led the charge, given the increased exposure to tornadoes year round, other nations such as China, Japan, and Australia have increased their efforts to record and detect TC tornadoes. Despite these advancements, more work needs to be done globally to understand the TC environment conducive for tornadic activity. Recommendations for future forecasting and research for TC tornadoes include i) develop a comprehensive global tornado database to improve research and forecasting efforts; ii) apply innovative technology to detect tornadoes; and iii) conduct field campaigns to thoroughly sample TC tornado environments, particularly along coastlines.

Keywords: Tropical cyclone; Tornado; Typhoon; Forecasting

1. Introduction

Tropical cyclone (TC) tornadoes pose a distinct threat to life and property that typically concentrates away from the most intense gradient-wind and storm-surge effects of the TC core, based on 17 climatologies described in the review by Edwards (2012; hereafter E12). Tornadoes also can persist inland for up to a week as the TC decays (E12; Nowotarski et al., 2021). TC

* Corresponding author.
E-mail address: ben.green@noaa.gov (B.W. Green).

Peer review under responsibility of Shanghai Typhoon Institute of China Meteorological Administration.

Production and Hosting by Elsevier on behalf of KeAi

https://doi.org/10.1016/j.tcrr.2023.06.003

tornadoes generally are smaller, less damaging [i.e. F/EF0 based on the Fujita (Fujita, 1971; McDonald, 2001) and/or Enhanced Fujita scales (WSEC, 2006; Doswell et al., 2009); see Section 2.3 for more on the F and EF scales], and shorter-lived than their midlatitude counterparts (e.g., McCaul, 1991; Edwards, 2010). Still, they account for about 3% of all known U.S. TC fatalities (Rappaport, 2014). Supercells produce the vast majority of TC tornadoes, and in September (the peak month for TC activity in the Atlantic basin), most U.S. tornadic supercells are spawned by TCs (Edwards et al., 2012).

Despite the risks posed by TC tornadoes, this hazard has received substantially less research attention globally compared to other TC threats (e.g., nontornadic winds, heavy rainfall, and storm surge). The relative dearth in TC tornado research results from a combination of several factors. First, TC tornadoes are more favored in the subtropics and midlatitudes. Second, tornadoes are usually small in spatial scale and are only observed over land, or along the coast as waterspouts. Third, TC tornadoes and their associated damage are often either missed completely (hitting in remote areas without people and/or radar coverage), or obscured by other concurrent TC hazards.

TCs have been treated as a subset of the possible environments in which tornadoes form; that is to say, TC tornado research has followed the lead of broader tornado research. As detailed below, the history of TC tornado research and forecasting has evolved from being solely focused on climatological factors (in a TC-relative framework) to one which uses an ingredients-based approach – like that used for non-TC tornadoes – recognizing that every TC poses a unique level of tornado risk which evolves over time. TC tornado research historically has been skewed dramatically towards a U.S.-centric framework – although China has recently invested heavily in infrastructure (both human and technological) to study and record the phenomenon. As a result, this report is necessarily biased towards the U.S. point of view, but every effort has been made to provide a global perspective.

This report on TC tornadoes was originally presented at the Tenth International Workshop on Tropical Cyclones (IWTC-X) in Bali, Indonesia, in December 2022. The remainder of this review is organized as follows: first, an overview of the research into TC tornadoes will be provided. Then, operational considerations will be discussed, using the U.S. as an example (but not in a prescriptive sense) of a highly coordinated forecast-verification-recording system and highlighting the variety of challenges faced by different nations. A summary and conclusions are provided at the end.

2. Research

2.1. Global overview of TC tornadoes

By definition, TC tornadoes only occur over land (TC waterspouts have been observed near the coastline, but not in the middle of the open ocean). TCs (or their post-tropical remnants) have been reported to spawn tornadoes in the following nations: Australia, Bermuda, the Bahamas, China, Cuba, Fiji, Japan, Mexico, India, Philippines, Portugal, Samoa, and the United States. Of these nations, only China, Japan, and the United States have seen more than 10 TCs that produced tornadoes.

In the U.S., while TC tornado records have been extracted from the Storm Prediction Center (SPC) national dataset before 1995 (e.g., Verbout et al., 2007; Schultz and Cecil, 2009), they include fewer records per year, with a high rating bias, due to a lower rate of reporting for weak (F0-1) tornadoes before the WSR-88D Doppler radar network was fully deployed in the mid 1990s (E12). In the most recent 27 years (1995–2021), 2.3 times as many TC tornadoes overall have been recorded than in the 45-year period of 1950–1994 (Edwards and Mosier, 2022). This increase is largely attributable to more intensive warning-verification efforts, better radar detection of tornadic supercells by the WSR-88Ds (including from newer dual-polarization capabilities) than their reflectivity-only predecessors, greater damage-survey attention, and better documentation of tornadoes by storm spotters and media (E12).

China averages approximately 8 landfalling TCs each year (Li et al., 2004); Bai et al. (2020) found that about one third of TCs which made landfall in China from 2006 through 2018 produced tornadoes, with an average of 5 TC tornadoes per year. TC tornadoes in China are likely undercounted, however, partly due to (i) a radar network that, while growing, until recently had coverage gaps; (ii) a relatively short period of standardized recordkeeping for tornadoes; and (iii) tornado damage being obscured by other TC hazards. As is common elsewhere, TC tornadoes are often few in number [Typhoon Yagi in 2018 produced at least 12 tornadoes, the most from one TC in China since 2000 (Diao et al., 2019)] and typically weak [the strongest TC tornado in China – rated EF3 – was spawned on 4 October 2015 by Typhoon Mujigae and resulted in 7 deaths and 229 injuries in Guangzhou and Foshan (Bai et al., 2017; Huang et al., 2018)]. Fig. 1 shows the distribution of TC-spawned tornadoes recorded in China from 2006 through 2018 (Bai et al., 2020).

According to the Australian Bureau of Meteorology (BoM), tornadoes have been reported with 3 TCs (Ita in 1997, Anthony and Carlos in 2011), plus 3 post-tropical cyclones (Ostwald in 2013, Marcia in 2015, and Debbie in 2017). Of note, 8 tornadoes were associated with Ex-Tropical Cyclone Ostwald, causing notable damage to property – including from one F3 tornado (the Enhanced Fujita scale, discussed in Section 2.3, is not used in Australia [Allen et al., 2021]) – in the Wide Bay region of Queensland. Additionally, tornadoes have been associated with tropical lows that never reached tropical cyclone status. Given limited dual-polarization (and, to a lesser extent, Doppler) radar coverage and sparse population in northern Australia, BoM records may be missing some TC tornado cases.

Regardless of less-than-ideal records, it is likely that the U.S., followed by China, has substantially more TC tornadoes than anywhere else in the world. These two countries have large areas of land vulnerable to TC strikes and are located in the midlatitudes; as discussed below, large-scale vertical wind shear induced by upper-level midlatitude westerlies are conducive (but by no means sufficient) for tornado formation.

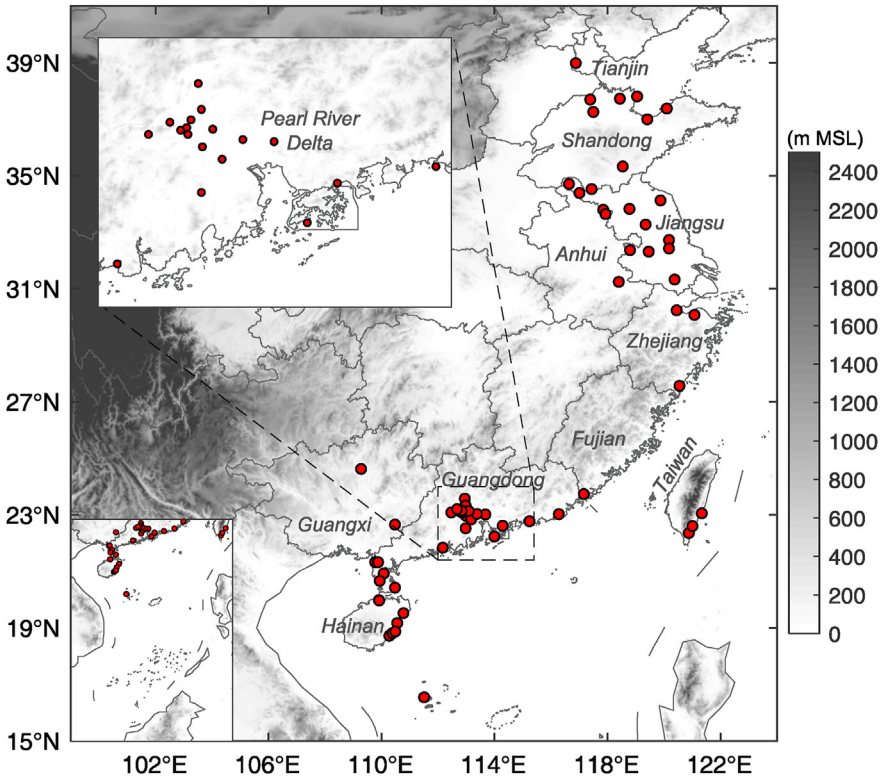

Fig. 1. Locations of TC tornadoes (red dots) in China from 2006 to 2018. The region around the Pearl River Delta is enlarged in the top-left corner. Terrain heights (in shading) are also shown for reference. From Fig. 2 of Bai et al. (2020), reproduced with permission from Springer Nature, http://springer.com/journal/11430.

2.2. Climatological distribution of tornadoes in TC-relative frameworks

Well into the 1980s, the environmental ingredients necessary for tornadic supercells – described in Section 2.3 – were poorly understood. Therefore, TC tornado research was limited to climatological studies that aimed to identify favorable locations within the TC envelope that were favorable for tornadogenesis. This research was confined to the Northern Hemisphere: specifically, the United States and Japan (e.g., Malkin and Galway, 1953; Smith, 1965; Pearson and Sadowski, 1965; Hill et al., 1966; Fujita et al., 1972). The main finding from these studies was that tornadoes tended to cluster in a sector primarily in the right-front quadrant (relative to TC forward motion) or northeast (relative to due north). These sectors often have significant overlap because TCs in the U.S. and Japan have a strong northward component of motion. However, the dangers of relying on such climatologies – particularly those using a TC forward-motion framework – were revealed in the case of Hurricane Beulah (1967); the TC spawned over 100 tornadoes in its rear quadrants, which happened to still be northeast of center due to a southwestward motion (Orton, 1970). In China, where TCs often translate toward the northwest, tornadoes tend to be concentrated in the northeast quadrant rather than the right-front quadrant (Bai et al., 2020). Larger TCs may yield more tornadoes, given their greater areal coverage of favorable environments (Paredes et al., 2021). In linking climatological TC tornado distributions to environmental parameters, Sueki and Niino (2016) showed that tornadic TCs (compared to non-tornadic TCs) had greater convective available potential energy [considering the effects of entrainment, E-CAPE (Zhang, 2009)] and storm-relative environmental helicity (SREH) in the northeast quadrant. CAPE and SREH are known to be key parameters for tornado development (Fig. 2). In effect, TCs are a special class of mesoscale convective system whose tornado distributions have physical bases in climatology, but these distributions vary according to their size, structure, and internal and external environments. Each TC, therefore, must be treated as its own unique and evolving tornado threat using the ingredients-based approach.

2.3. TC tornadoes within the ingredients-based framework

The climatological concepts discussed above form a baseline understanding of TC tornado occurrence for forecasting, though any given cyclone may deviate substantially in terms of more-focused sectors within the broader, climatologically favored north-to-southeast swath (in the southern hemisphere, assuming the physical processes are spatially mirrored as with other weather systems, the favored sector for tornadoes would be south-southwest through southeast and northeast of TC center [E12]). Some TCs produce no tornadoes, while others of similar intensity/size/track spawn over 100 (E12). Therefore, an improved understanding of TC tornadoes must not treat the

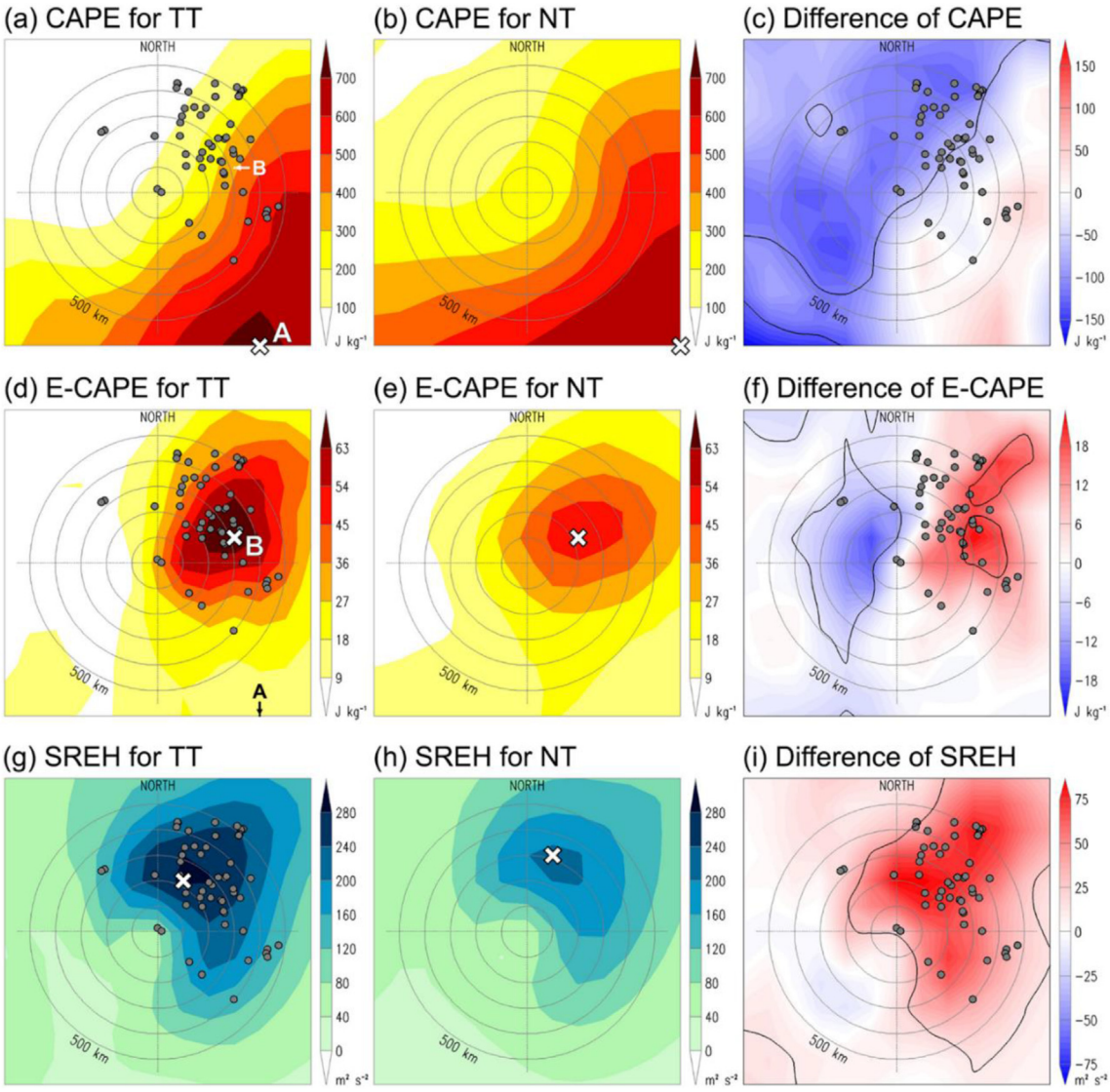

Fig. 2. Composite horizontal distributions of (a–c) CAPE, (d–f) E-CAPE, and (g–i) SREH around the typhoons used in the study of Sueki and Niino (2016). The left and middle columns are for tornadic typhoons (TT) and non-tornadic typhoons (NT) respectively; the right column shows the difference between the two (TT minus NT). Locations of maximum values within the displayed area are shown by the cross marks in the panels of TT and NT. The areas in which the difference between TTs and NTs are statistically significant at 5% based on Welch's *t*-test are enclosed by solid black lines in the right column. Solid gray circles in the left and right columns show locations of tornadoes relative to the typhoon centers. From Fig. 1 of Sueki and Niino (2016).

TC as a monolithic entity, but instead consider the environments within the TC that are favorable for tornadogenesis. This understanding is rooted in the numerous studies of "supercell" thunderstorms: discrete cellular convection with rotating updrafts. Tornadic supercells form in environments with sufficient buoyancy, vertical wind shear, and a low level of free convection (McCaul et al., 2018).

These supercell-favoring ingredients also are no different in TCs than for midlatitude supercells. The TC environment, however, characteristically features *different relative distributions* of them. A landfalling TC is typified by large wind shear and high moisture content while thermodynamic instability (e.g., CAPE) is limited primarily due to evaporative cooling and decreased solar radiation induced by cloud cover. Using a number of proximity rawinsonde observations, McCaul (1991) found that the average CAPE is 253 J kg^{-1} for TC tornado environments in the United States – substantially lower than the average CAPE for non-TC tornado environments. However, CAPE may also sometimes be boosted diurnally by overland insolation in midtropospheric dry-air intrusions (e.g., Curtis, 2004; Baker et al., 2009). Regardless, TC tornado occurrence maximizes in the mid-to late afternoon, suggesting that instability is still an important ingredient for tornadogenesis (McCaul, 1991; Schultz and Cecil, 2009). Because of the inherent abundance of moisture in TCs, the key factors that control tornado occurrence are the juxtaposition of instability and wind shear as well as the necessary forced lift to initiate storms. The extremely high shear (and helicity) and low-buoyancy environment, with a relatively lower equilibrium level, is conducive for low-topped "miniature" supercells

(Fig. 3), the predominant convective storm type for TC tornadoes (McCaul and Weisman, 1996; Edwards et al., 2012). Not surprisingly, the distributions of supercells (mesocyclones) and tornadoes within TCs are nearly identical (cf. Fig. 3 of Bai et al., 2022) – the highest concentrations are in the northeast quadrant (for the northern hemisphere).

The presence of (miniature) supercells in TCs is not sufficient for tornadoes. While the exact mechanisms of tornadogenesis (i.e., creating a violently rotating column of air from cloud base all the way to the ground) remain elusive, a supercell crossing a horizontal baroclinic boundary may be more likely to spawn a tornado (Edwards and Pietrycha, 2006). These baroclinic boundaries may arise from synoptic-scale fronts or mesoscale outflow boundaries. The coastline provides a natural boundary, with stronger horizontal temperature gradients and higher low-level shear over land (Gentry, 1983; Green et al., 2011). Indeed, many U.S. TC tornadoes occur right along the coastline (Fig. 4).

Areas of favorable lift are interdependent with influences of deep-tropospheric shear on the TC envelope. When TCs interact with midlatitude troughs, the latter's enhancements of both deep shear and shallow, low-level shear favor TC tornadoes (Verbout et al., 2007). Sufficiently deep and sustained convection with potential to become tornadic supercells typically is distributed asymmetrically to approximately the eastern half of the TC circulation. This setting arises via impositions of ambient deep-tropospheric (i.e., 850-200-hPa), typically (in the northern hemisphere) southwesterly to westerly vertical wind shear on the landfalling to inland convective distribution and environmental parameter space (Schenkel et al., 2020; 2021). Somewhat consistent with the presence of a natural boundary along the coastline, Schenkel et al. (2021) found that coastal tornadoes occur regardless of deep shear magnitude, whereas inland tornadoes primarily occur in strongly sheared TCs. The schematic in Fig. 5 offers a conceptual model of the deep-shear influence and tornado-favoring, TC-scale convective asymmetries. Stronger ambient deep shear (especially in larger TCs; Paredes et al., 2021) in turn boosts TC tornado potential by supporting larger, longer-lived convective development in favorable parameter spaces of CAPE and enlarged lower-tropospheric hodographs.

From 2007 to the present, U.S. tornadoes have been rated on a 0–5 scale, 5 being the worst destruction level, based on the Enhanced Fujita (EF) scale (Edwards et al., 2013) which uses subjective assessments of damage intensity to 21 types of structures and trees, to assign probable ranges of wind speeds at sites along a tornado path. Prior to 2007, the U.S. used the similarly six-level, nominally house-based Fujita (F) scale. In TC settings, some tornado damage also may be obscured, enhanced, or removed altogether by subsequent wind and/or hydraulic impacts (i.e., storm surge, freshwater flooding). Still, F and EF ratings constitute *coarse estimates* of tornado intensity that have proved useful and practically ubiquitous in bulk climatological analyses of tornadoes, including TC tornadoes (E12). Most TC tornadoes are rated in the "weak" segment of the scales, at F/EF0-1 (Table 1).

3. Operational considerations

3.1. Current operational procedures for forecasting, observing, and verifying TC tornadoes

Operational practices for TC tornadoes vary widely by nation. The reasons for the variability are a combination of (i) bureaucratic organization; (ii) coverage provided by remote sensing platforms [radar]; and (iii) frequency of tornadoes, TC or otherwise. For example, Australia rarely experiences tornadoes, and the main region that sees TC tornadoes – northern

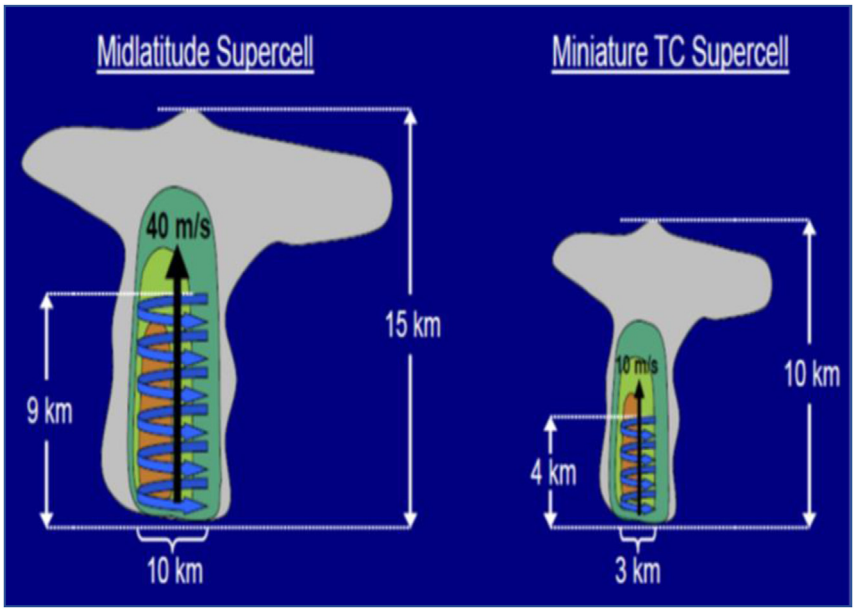

Fig. 3. Schematic of a midlatitude supercell (left) and shallow "miniature" TC supercell (right). From Eastin et al. (2012); used with permission.

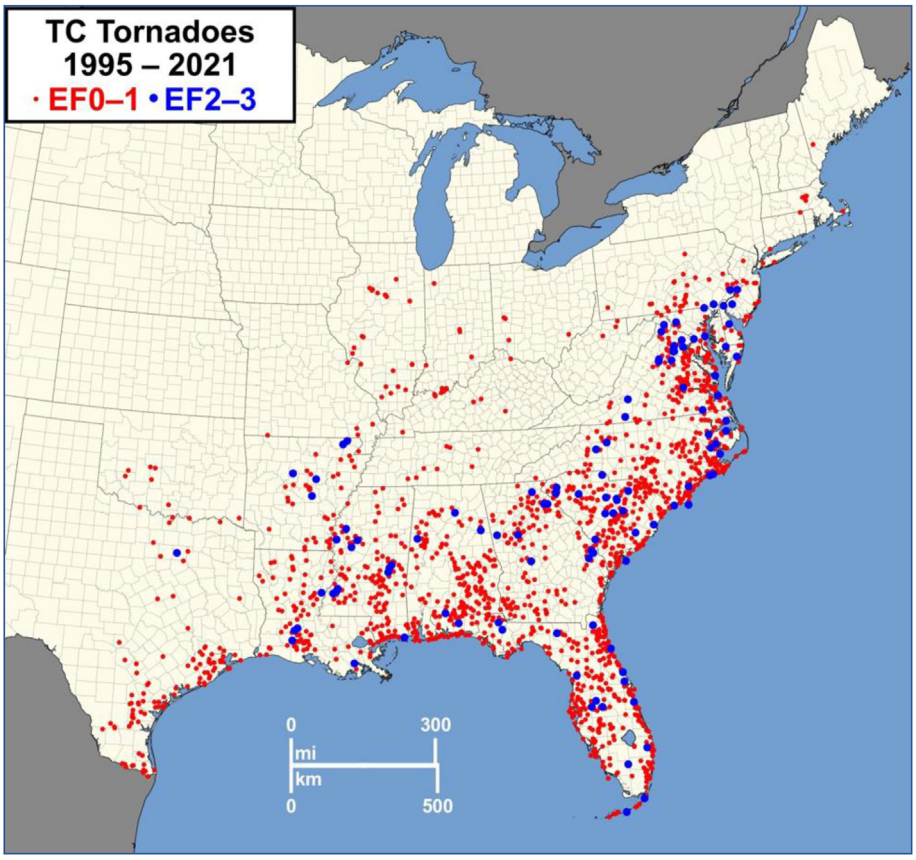

Fig. 4. Map of 1746 U.S. TC tornadoes, 1995–2021, rated F/EF0-1 (red dots) and F/EF2-3 (blue dots). No F/EF4-5 tornadoes occurred. From Fig. 4 of Edwards and Mosier (2022).

Australia – is sparsely populated and has limited radar coverage (the areas covered by Doppler radar and dual-polarization radar are smaller still). The Australian BoM employs the same general tornado forecasting techniques for TC situations as they do for non-TC situations, although the gaps in dual-polarization radar, Doppler radar, or even older reflectivity-only radar over remote inaccessible areas can make verifying TC tornadoes challenging or impossible.

China – like Australia – currently has limited (dual-polarization) Doppler radar coverage, although there are ongoing efforts to rapidly expand their radar network, particularly in areas prone to TC tornadoes. Tornado warnings in general are a relatively new product in China: the Chinese Meteorological Administration began testing tornado warnings in October 2016 in some provincial meteorological departments. Guandong Meteorological Service has deployed more than 30 X-band dual-polarization phased array radars in the highly populated Pearl River delta; other provincial departments are building X-band Doppler radar networks. In 2018, Guandong became the first (and, as of 2022, remains the only) province to issue warnings for TC tornadoes. On a larger scale, forecasters use an ingredients-based approach (e.g., environmental shear, helicity, instability, etc.) from numerical model output to assess the risk for TC tornadoes; if the risk is high, the threat is communicated to the public through media channels. Meteorological observatories in Chinese cities often collaborate with each other on TC tornado warnings and verification.

The United States has by far the most sophisticated, coordinated, end-to-end process for TC tornado forecasting, warning, verification, and record-keeping. This is because the U.S. experiences tornadoes almost year-round, with an additional contribution from TCs in late boreal summer through autumn, over large areas of relatively dense population. As detailed in the following paragraphs, TC tornado forecasting in the U.S. follows the pattern of the broader "forecast funnel" in which forecasts become more generic outward through time.

If the TC is still well offshore, not posing a tornado threat in the next several hours, it falls in the "outlook" timeframe (~12 h–~3 days). Diagnostics then are broader-scale, mainly synoptic (1000s of km) in nature, involving pattern analysis, recognition and understanding. That often includes upper-air analyses and concurrent examination of multi-channel satellite imagery for all severe-local-storm threats across the U.S., including from the forthcoming potential TC landfall. Track and intensity guidance provided by the National Hurricane Center (NHC) is the most important part of the latter scenario, given the importance of consistency with the expert (NHC) TC forecast in messaging the threat timing and location, as applied to the tornado threat. Synoptic-scale, operational numerical models always are examined for the broader severe-weather

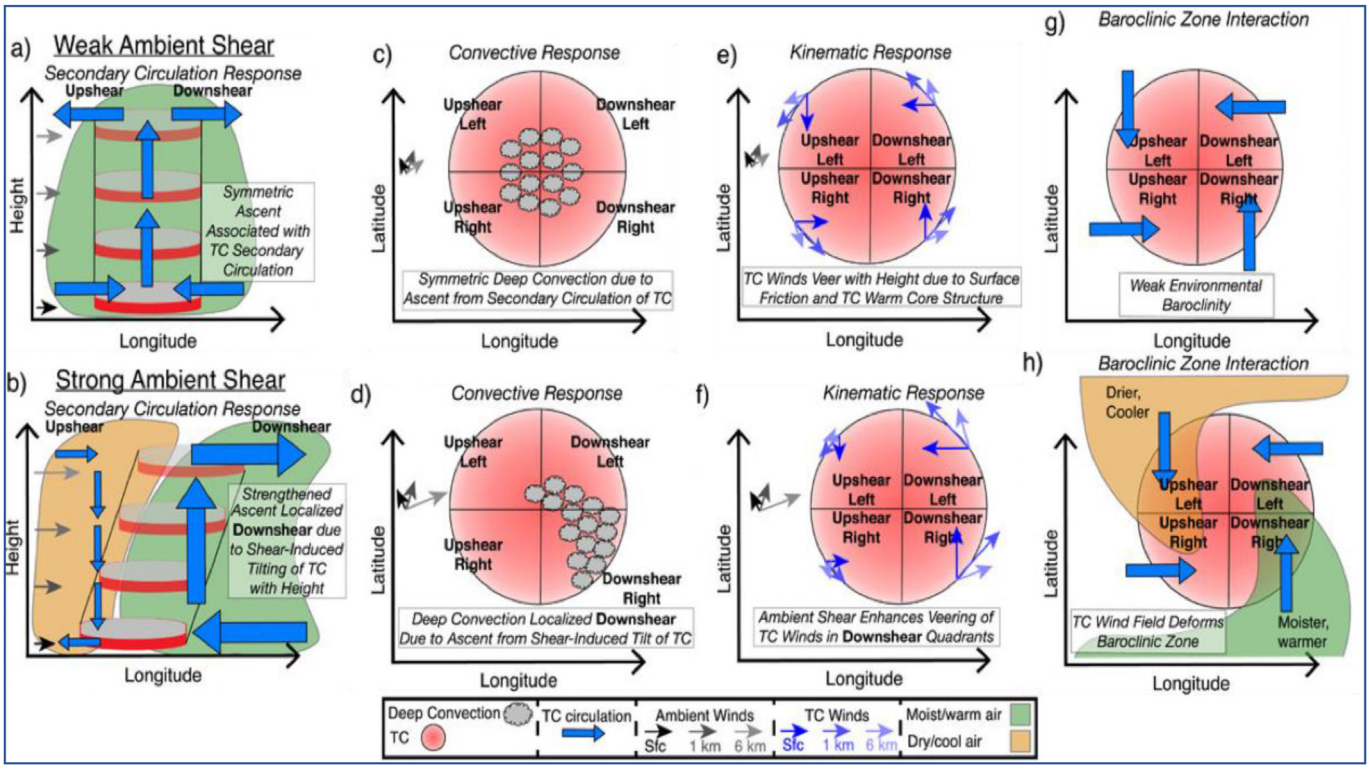

Fig. 5. Schematic of influence of ambient 850-200 hPa vertical wind shear on a potentially tornadic TC in weak (top row, lowest tercile, <6.7 m s^{-1} vector magnitude) and strong (bottom column, highest tercile, >11.2 m s^{-1} vector magnitude) shear: (a,b) Vertical tilt from secondary circulation response; (c,d) Horizontal convective distribution; (e,f) Kinematic response; (g,h) Baroclinic interaction response. Adapted from Fig. 2 of Schenkel et al. (2020). © American Meteorological Society. Used with permission.

Table 1
U.S. TC tornado percentages by F/EF-scale rating, 1995–2021. EFU (unknown) is a relatively new category – seldom used in practice – representing tornadoes occurring in inaccessibly remote and/or undeveloped areas where damage is undocumented, or damage indicators are not present. Data is taken from the TCTOR database maintained by the SPC, as detailed in Section 3.1.

F/EF-scale rating	U	0	1	2	3
% U.S. TC tornadoes, 1995–2021	0.3%	64.0%	29.4%	6.0%	0.3%

potential nationwide, but NHC forecasts take priority on the rare occasions when differences appear. Beyond 24 h of the first TC tornado threat, tornado outlook areas are drawn largely using climatology and NHC predictions of TC size, intensity and track. As the TC approaches landfall (within 24 h of its outermost bands potentially affecting the coastline), the forecast funnel narrows and deepens into the subsynoptic, with more specific environmental interrogation. The environmental factors considered are moisture, instability (e.g., CAPE), vertical shear (both deep and near-surface), and sources for lift. Whether for TC or non-TC supercells, these ingredients do not follow rigid operational thresholds individually, because their favorability for tornadoes exists in dependent balance with the others.

Mesoscale timescale forecasting (next several hours) of TC tornado environments involves both manual and automated diagnostic techniques in the United States. This still necessarily includes subjective hand analyses of printed maps in the operational setting, to optimize a forecaster's immersive situational understanding. Specific to TCs, manual and objective surface analyses, combined with satellite imagery, soundings, hodographs (including from overland radar-derived winds), and radar base-data displays, help to diagnose subtle kinematic and baroclinic boundaries within the TC that may maximize the overlap of buoyancy and low-level shear favorable for tornadic supercells (Edwards and Pietrycha, 2006). Signs of potential supercell development, especially when the environment downstream (with respect to expected cell motion) contains a favorable boundary, may be highlighted for SPC-issued tornado watches or short-fused mesoscale discussions. Great caution must be exercised extrapolating *diagnostic* supercell- and tornado-favorable parameters out in *prognostic* time (Doswell and Schultz, 2006), including in the continually evolving TC setting. Base diagnostic variables (temperature, moisture, wind) still matter most analytically.

Because TC supercells tend to be shallower, narrower, and less resolvable at similar distances from radars compared to their midlatitude counterparts (e.g., McCaul and Weisman, 1996; McCaul et al., 2004; E12), timely radar detection of their tornadic mesocyclones has proved more difficult (e.g., Spratt et al., 1997; Schneider and Sharp, 2007), especially with greater distance. For those reasons, TC tornado warnings typically have had higher false-alarm ratios than their midlatitude counterparts in the United States (e.g., Martinaitis, 2017; Nowotarski et al., 2021) and in China. Radar

reflectivity presentations for tornadic TC supercells span a large spectrum, from those with hook echoes upshear from forward-flank cores (as with many midlatitude supercells), to quite messy and indistinct (e.g., Spratt et al., 1997; Schneider and Sharp, 2007; Edwards and Picca, 2016). Nonetheless, even tornadic TC supercells with nebulous reflectivity signatures often display the same velocity characteristics as those in midlatitudes, just smaller in scale – including well-defined, persistent mesocyclones. For supercells where radar observations are distant, noisy or unavailable, lightning data have proven useful in assessing strengthening trends as precursors to tornadogenesis (e.g., McCaul et al., 2004). Given a general dearth of lightning in TCs compared to midlatitude thunderstorm complexes, the presence of *any* detected lightning in outer-band cells may draw attention to their hazard potential (Schultz et al., 2011). Relatively deep, intense cells also should have cooler cloud tops on infrared satellite imagery. As such, when cells in climatologically and environmentally favorable TC sectors are far from radars (including still well offshore, but moving toward land), attention to tornado potential should be heightened by the persistence of high or increasing radar-echo tops, anomalously prolific or increasing lightning production, and anomalously cold or rapidly cooling cloud tops.

In the United States, the retrofitting of the existing 10-cm-wavelength WSR-88D network with dual-polarization capabilities, along with enhanced-resolution scanning strategies at lower elevations, has allowed explicit detection of tornadic debris signatures (TDSs; Rhyzhkov et al., 2005) via the cross-correlation coefficient (ρ_{HV}) product. Although the TDS can only appear after tornadogenesis, its presence essentially confirms to the warning forecaster that a cell is tornadic and increases confidence in downstream warnings, given a favorable environment and persistence of other indicative radar signatures. A TDS also gives approximate but reliable timing and location information for later targeting by damage surveyors, including in remote areas. As such, the TDS offers more tornadic confirmation capabilities, and has added TC tornado events to databases like TCTOR (detailed below) that otherwise may have gone unrecorded. The benefits of the TDS perhaps are most pronounced in TCs, where the prevailing mass of warm-cloud raindrops and lack of hail often present a nearly homogeneous ρ_{HV} field. Within that setting, the much more reflective and asymmetric debris can stand out brilliantly (Edwards and Picca, 2016). Fig. 6 presents an archetypical example of a TC TDS in an otherwise challenging warning situation, with a large and chaotic reflectivity echo, weak but apparent mesocyclone, and readily apparent, co-located ρ_{HV} minimum. Deployment of dual-polarization radar presents tremendous promise in TC tornado detection, and nations such as Australia and China are working to expand dual-polarization coverage.

Forecast responsibility for TC tornadoes in the U.S. is delegated largely by timescale, with the SPC handling areal responsibility across the entire TC envelope and near/overland lifespan. SPC outlooks, which are composed of areal threat or "risk" graphics and textual reasoning, forecast the unconditional probability of an event (such as a TC tornado) within about 40 km of any point in the outlook areas. Those probabilities drive differently colored "risk" areas categorically labeled. "High risks" have never been used for TC tornadoes and "moderate risks" in TCs are exceedingly rare – most TC tornado outlooks are "enhanced" or lower equivalent probabilities. The generalized SPC national outlooks issued in the day-4 through day-8 (after the current day) period, for ≥15% probabilities, never have included TCs graphically, and at most only offer superficial text mention. This is because of the mesoscale nature of TC tornado production and uncertainties inherent to TC track and intensity forecasting at that timeframe. Those uncertainties generally resolve through day 3 (day after tomorrow, when the lowest probability is 5%) and day 2 (tomorrow, lowest probability has become 2%). Greater unconditional certainty with nearer time allows more TC tornado outlook areas to appear. Day-2 and day-1 (same-day) outlooks explicitly forecast tornado threat and assign category levels to ascending tornado-only probabilities for TCs. As the TC approaches landfall, SPC begins participating in a videoconference with NHC and other affected National Weather Service (NWS) offices, which includes diagnostic and forecast insights on all other TC hazards. The tornado potential is coordinated to inform NHC public bulletins and NWS messaging needs.

On day 1, within a few hours of the onset of an overland TC tornado threat, SPC will begin issuing mesoscale discussions of TC tornado potential. Mesoscale discussions are shorter than outlooks in text length, but more finescale spatiotemporally, with a graphical component highlighting the threat area. Mesoscale discussions initially precede each TC tornado watch, but are issued at least once (usually more) during the valid time of a watch, as an update to the meteorological setting of the threat potential. They also may be issued to inform of a marginal, small-scale and/or brief tornado threat that does not warrant a watch.

SPC tornado watches outline areas of relatively maximized tornado potential within the ensuing several hours, in the projected path of the most-favorable TC sector. Most TC tornado watches last 8–15 h given the gradual evolution of the TC tornado threat; however, watches can target smaller areas and blocks of time down to just 2–3 h as needed. SPC watches are coordinated via conference call with affected local NWS offices.

Local NWS weather forecast offices tailor SPC forecasts graphically to their jurisdictions at all timescales, and issue tornado warnings. TC tornado warnings typically occur in polygons tens to hundreds of km^2 in area, starting at the initial location of the hazardous cell, extending along the projected motion for the next 15–45 min, and gradually spreading laterally from that vector with time to account for cell-translation uncertainty. These warnings are based on some combination of radar signals (cf. Fig. 6) and eyewitness reports.

Within three months after a TC, local NWS offices send a listing of its confirmed tornadoes to NWS headquarters, for aggregating and input to National Centers for Environmental Information's (NCEI) *Storm Data* publication. Shortly after the calendar year ends, SPC collects all *Storm Data* reports nationally, including from TCs, and creates whole tornado paths

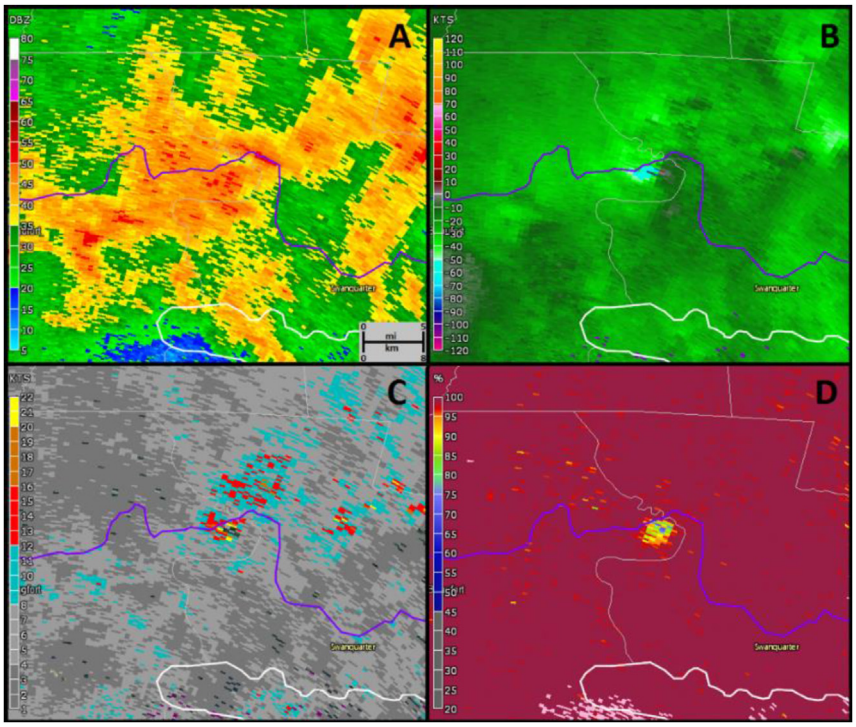

Fig. 6. Planar (0.5° beam elevation) display of TC Irene products from Morehead City, US WSR-88D, 0203 UTC 27 August 2011: (a) base reflectivity, (b) base velocity, (c) spectrum width, (d) ρ_{HV}. Values and units as shown in scales. Tornado was near the center of each panel and northeast of the radar, moving generally westward (right-to-left). Purple curve is U.S. Highway 264. From Fig. 2 of Edwards et al. (2015). Mapping courtesy GRLevel2®.

for a unified tornado database (Schaefer and Edwards, 1999) and provides the dataset freely and publicly (https://www.spc.noaa.gov/wcm/#data; last accessed 8 February 2023). This dataset includes F/EF ratings, path length, maximum width, event-tracking numbers, states, as well as start and end data (latitude, longitude, date, and time [U.S. Central Standard Time]). From this dataset, SPC distills a TC tornado subset that is also provided to the public domain (TCTOR; Edwards, 2010; https://www.spc.noaa.gov/publications/edwards/tctor.xls; last accessed 8 February 2023) along with an accessory file featuring documentation and updates (https://www.spc.noaa.gov/publications/edwards/readme.txt; last accessed 8 February 2023). TCTOR also includes a common metric of path-based tornado-impact potential known as the destruction potential index (DPI; Thompson and Vescio, 1998), tornado-contemporaneous TC track and intensity data presented in version 2 of the NHC North Atlantic hurricane dataset (HURDAT2; Landsea and Franklin, 2013). The HURDAT2 information is used to compute tornadogenesis azimuth and range points from interpolated TC center fixes; the resulting data (in north-relative and TC-motion-relative frameworks) also are included in TCTOR. As of this writing, TCTOR includes 1746 known tornadoes in the conterminous U.S. from 1995 to 2021. Over the past decade, TCTOR has become the standard research climatology for U.S. TC tornadoes (e.g., Schenkel et al., 2020; 2021; Nowotarski et al., 2021; Paredes et al., 2021).

In general, nations survey TC tornadoes using whatever protocols they have developed to survey non-TC tornadoes. However, as mentioned in Section 2.3, TC tornado damage may be obscured (or enhanced) by other TC hazards. Thus, within a given nation, there may be considerable variance in surveying TC tornado damage depending on the amount of real-time data (radar, video) and accessibility (remoteness, obstructions caused by other TC hazards). In some cases where a TC tornado strikes a populated area and considerable real-time data are available, a meticulous damage survey can be performed (e.g., Bai et al., 2017).

3.2. Best practices for communicating TC tornado risk

At the BoM, hazards are assessed separately, with each having associated community actions for individual risk thresholds. These community actions are often combined in a single warning product. In the case of TC tornadoes, generally these are a lower risk, both in regards to their rarity in Australia and the broader risk from other TC hazards (including rainfall and storm tide) usually being a more significant priority. Given this, standard practice is to emphasize the most significant hazards, with risk of tornadoes generally a footnote.

In the U.S., tornado warnings (regardless of whether or not they are associated with a TC) also have a text component with timing, hazard and location information provided in a consistent format for ready use by media and emergency officials, and activate National Oceanic and Atmospheric Administration (NOAA) weather radio, emergency broadcast functions on traditional media, social media, and most recently, automated emergency messages sent to smartphones. NWS (TC) tornado

warnings are impact-based warnings, and can be assigned "base," "considerable," or "catastrophic" damage tags based on the perceived impact (the presence of a TDS on radar would merit at least a "considerable" damage tag).

Sometimes tornado and flood threats overlap (Henderson et al., 2020, Fig. 7 for a U.S. TC tornado example), prompting potential confusion and even contradiction in emergency messaging. For example, standard advice for tornado sheltering, in the interior lowest level of a building, can be dangerous when the ground floor submerges in floodwaters, as happened in Hurricane Harvey in 2017 (Nowotarski et al., 2021), or in storm surge. Damaging non-tornadic winds – whether from gradient flow in the TC or embedded cells – also can overlap areas with imminent flood and tornado dangers.

3.3. Current operational limitations and future developments

In both Australia and China, for example, coverage of dual-polarization Doppler radar remains limited, thus hampering the ability to detect, warn, and verify TC tornadoes. Both nations are investing in upgrades to their radar networks (although there will still be gaps in dual-polarization coverage over northern Australia for the foreseeable future). There is ongoing work by the BoM to develop and implement an Australian Warning Service that is a combination of hazard assessment and the total impact to the community. This tiered approach aims to better communicate actual risk from any severe weather regardless of source. Similarly, in the U.S., efforts are

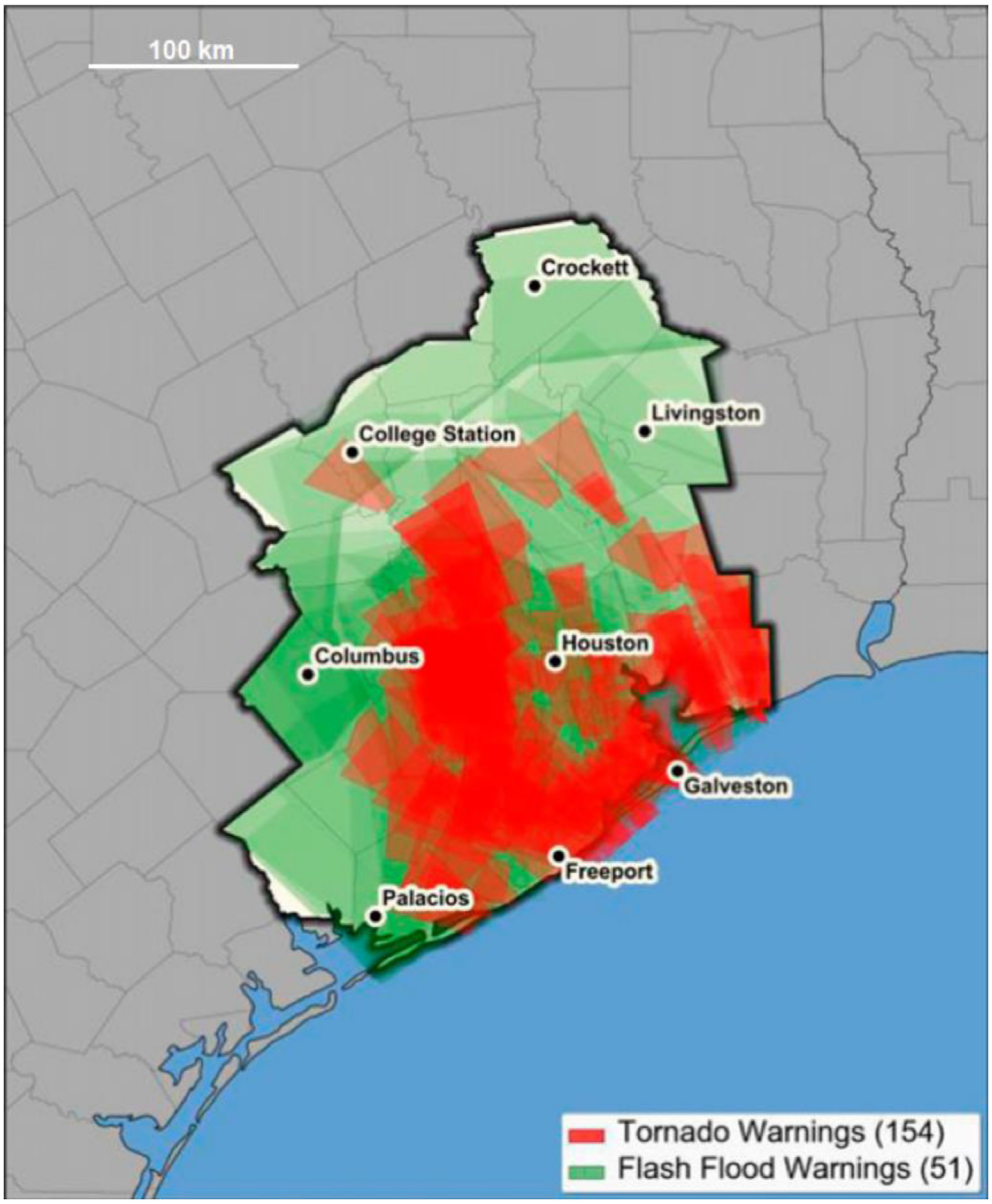

Fig. 7. Overlaid polygonal tornado (red) and flash flood (green) warnings issued within the jurisdiction of the Houston-Galveston NWS office (black outline) during Hurricane Harvey, 1200 UTC 25 August 2017–1200 UTC 27 August 2017. Deeper shading means more of that warning type at a given location, with tornado warnings taking priority here. From Figure 10 of Nowotarski et al. (2021). © American Meteorological Society. Used with permission.

underway in the NWS to develop more specific and clearer threat messaging for TC situations where multiple, potentially deadly, short-fused hazards affect a single locale within a TC. China is still in earlier stages of developing robust (TC) tornado prediction and warning protocols in terms of making forecasts and issuing/verifying warnings.

In various nations, there is increasing reliance on high-resolution (convective permitting) numerical model guidance for short-fused hazardous weather warnings, including (TC) tornadoes. In 2022, Australia operationally implemented its Access-C convective allowing model centered on Townsville, Queensland, Australia; this will assist with forecasting TC tornadoes over one of the more densely populated regions of northern Australia. In the U.S., such models have been integrated into severe-storms forecasting operations at SPC since around 2010. These typically are variations of the Weather Research and Forecasting (WRF; Skamarock et al., 2008) or the High Resolution Rapid Refresh (HRRR; Benjamin et al., 2016), and can assimilate radar and observed mesoscale observational data for hourly runs. In midlatitude severe-weather situations, this guidance already is operational, offering explicit forecasts of convective modes through post processed displays of strong and sustained cell-scale corridors of updraft helicity (Kain et al., 2008) co-located with simulated echoes that appear as supercells would on radar. Such models, which also offer mesoscale environmental fields pertinent to supercell forecasting, often are examined in TC-tornado scenarios, but their fidelity and accuracy have not been systematically tested in TCs.

4. Summary and conclusions

Tornadoes are one of the many hazards to life and property posed by TCs. Although TC tornadoes are generally weaker than non-TC tornadoes and most commonly occur in the United States and China, they do pose a global threat. The majority of TC tornadoes are produced by shallow-topped "miniature" supercells, and occur in the northeastern quadrant of the TC (in the northern hemisphere) due to a climatological preference for enhanced instability and shear in that region. However, an improved understanding of the ingredients for tornadogenesis (e.g., instability and shear) shows TC tornado forecasting to be more successful when the TC is treated as a time-evolving large-scale forcing rather than a static, monolithic entity. The U.S. has a well-established protocol to forecast, detect, warn, verify, and document/record TC tornadoes. Other nations are working towards the lead of the U.S., but are currently limited by (i) the relatively rare occurrence of TC tornadoes and (ii) gaps in dual polarization Doppler radar coverage. Social media can also be a useful tool to collect images/videos of TC tornadoes from the public in real-time. In the absence of radar coverage and/or real-time reporting, operational meteorologists may consider the use of lightning products on high-resolution satellite imagery, combined with knowledge of the abovementioned ingredients-based framework, to identify regions of heightened TC tornado potential. Communicating the risk of TC tornadoes to the public can lead to confusion given the abundance of concurrent hazards, and in the case of flooding, can result in directly contradictory advice. The impacts of climate change on the global distribution of TC tornadoes are unknown.

Acknowledgments

Dr. Benjamin Schenkel is thanked for proposing the topic of TC tornadoes to the TC hazards group of IWTC-X, and for helping to recruit the authors of this article. Matt Eastin is thanked for giving permission to use Fig. 3. Fig. 1 is used with permission from Springer Nature. Figs. 5 and 7 are © American Meteorological Society and used with permission.

References

Allen, J.T., Allen, E.R., Richter, H., Lepore, C., 2021. Australian tornadoes in 2013: implications for climatology and forecasting. Mon. Wea. Rev. 149, 1211–1232. https://doi.org/10.1175/MWR-D-20-0248.1.

Bai, L., Meng, Z., Sueki, K., Chen, G., Zhou, R., 2020. Climatology of tropical cyclone tornadoes in China from 2006 to 2018. Sci. China Earth Sci. 63, 37–51. https://doi.org/10.1007/s11430-019-9391-1.

Bai, L., Meng, Z., Zhou, R., Chen, G., Wu, N., Wong, W.-K., 2022. Radar-based characteristics and formation environment of supercells in the land-falling Typhoon Mujigae in 2015. Adv. Atmos. Sci. 39, 802–818. https://doi.org/10.1007/s00376-021-1013-2.

Bai, L., Meng, Z., Huang, L., Yan, L., Li, Z., Mai, X., Huang, Y., Yao, D., Wang, X., 2017. An integrated damage, visual, and radar analysis of the 2015 Foshan, Guangdong, EF3 tornado in China produced by the land-falling Typhoon Mujigae (2015). Bull. Amer. Meteorol. Soc. 98, 2619–2640. https://doi.org/10.1175/BAMS-D-16-0015.1.

Baker, A.K., Parker, M.D., Eastin, M.D., 2009. Environmental ingredients for supercells and tornadoes within Hurricane Ivan. Wea. Forecast. 24, 223–244. https://doi.org/10.1175/2008WAF2222146.1.

Benjamin, S.G., Weygandt, S.S., Brown, J.M., Hu, M., Alexander, C.R., Smirnova, T.G., Olson, J.B., James, E.P., Dowell, D.C., Grell, G.A., Lin, H., Peckham, S.E., Smith, T.L., Moninger, W.R., Kenyon, J.S., Manikin, G.S., 2016. A North American hourly assimilation and model forecast cycle: the Rapid Refresh. Mon. Wea. Rev. 144, 1669–1694. https://doi.org/10.1175/MWR-D-15-0242.1.

Curtis, L., 2004. Midlevel dry intrusions as a factor in tornado outbreaks associated with landfalling tropical cyclones from the Atlantic and Gulf of Mexico. Wea. Forecast. 19, 411–427. https://doi.org/10.1175/1520-0434(2004)019<0411:MDIAAF>2.0.CO;2.

Diao, X.G., Meng, X.G., Zhang, L., Ren, Z.D., Zhao, H.J., 2019. Analysis of microscale vortex signature and early warning capability of tornadoes in the circulations of typhoons Yagi and Rumbia. J. Mar. Meteorology 39, 19–28 (in Chinese).

Doswell III, C.A., Schultz, D.M., 2006. On the use of indices and parameters in forecasting severe storms. Electron. J. Severe Storms Meteorol. 1, 1–22. https://doi.org/10.55599/ejssm.v1i3.4.

Doswell III, C.A., Brooks, H.E., Dotzek, N., 2009. On the implementation of the enhanced Fujita scale in the USA. Atmos. Res. 19, 554–563. https://doi.org/10.1016/j.atmosres.2008.11.003.

Eastin, M.D., Hays, B.M., Link, M.C., 2012. Discriminating between tornadic and non-tornadic soundings in tropical cyclones. In: 30th Conf. On Hurricanes and Tropical Meteorology. Amer. Meteor. Soc., Ponte Vedra Beach, FL. P1.6. https://ams.confex.com/ams/30Hurricane/webprogram/Paper205037.html.

Edwards, R., 2010. Tropical cyclone tornado records for the modernized NWS era. In: Proc., 25th Conf. On Severe Local Storms. Amer. Meteor. Soc., Denver, CO. P3.1. https://ams.confex.com/ams/pdfpapers/175269.pdf.

Edwards, R., 2012. Tropical cyclone tornadoes: a review of knowledge in research and prediction. Electron. J. Severe Storms Meteorol. 7, 1–61. https://doi.org/10.55599/ejssm.v7i6.42.

Edwards, R., Mosier, R.M., 2022. Over a quarter century of TCTOR: tropical cyclone tornadoes in the WSR-88D era. In: Proc., 30th Conf. On Severe Local Storms. Amer. Meteor. Soc., Santa Fe, NM, USA. https://www.spc.noaa.gov/publications/edwards/27yr-sls.pdf.

Edwards, R., Picca, J.C., 2016. Tornadic debris signatures in tropical cyclones. In: Proc., 28th Conf. On Severe Local Storms, Portland, OR, USA. Amer. Meteor. Soc., p. P162. https://ams.confex.com/ams/28SLS/webprogram/Manuscript/Paper300633/tcttds.pdf

Edwards, R., Pietrycha, A.E., 2006. Archetypes for surface baroclinic boundaries influencing tropical cyclone tornado occurrence. In: Proc., 23rd Conf. On Severe Local Storms. Amer. Meteor. Soc., St. Louis, MO, USA. P8.2. https://ams.confex.com/ams/pdfpapers/114992.pdf.

Edwards, R., Dean, A.R., Thompson, R.L., Smith, B.T., 2012. Convective modes for significant severe thunderstorms in the contiguous United States. Part III: tropical cyclone tornadoes. Wea. Forecast. 27, 1507–1519. https://doi.org/10.1175/WAF-D-11-00117.1.

Edwards, R., LaDue, J.G., Ferree, J.T., Scharfenberg, K., Maier, C., Coulbourne, W.L., 2013. Tornado intensity estimation: past, present, and future. Bull. Amer. Meteorol. Soc. 94, 641–653. https://doi.org/10.1175/BAMS-D-11-00006.1.

Edwards, R., Smith, B.T., Thompson, R.L., Dean, A.R., 2015. Analyses of radar rotational velocities and environmental parameters for tornadic supercells in tropical cyclones. In: Proc., 37th Conf. On Radar Meteorology. Amer. Meteor. Soc., Norman, OK, USA, 5A.3. https://www.spc.noaa.gov/publications/edwards/vrot-tc.pdf.

Fujita, T.T., 1971. Proposed Characterization of Tornadoes and Hurricanes by Area and Intensity. University of Chicago SMRP Research, p. 42. Paper 91. https://archive.org/details/nasa_techdoc_19720008829.

Fujita, T.T., Watanabe, K., Tsuchitya, K., Shimada, M., 1972. Typhoon-associated tornadoes in Japan and new evidence of suction vortices in a tornado near Tokyo. J. Met. Soc. Jpn. 50, 431–453.

Gentry, R.C., 1983. Genesis of tornadoes associated with hurricanes. Mon. Wea. Rev. 111, 1793–1805. https://doi.org/10.1175/1520-0493(1983)111<1793:GOTAWH>2.0.CO;2.

Green, B.W., Zhang, F., Markowski, P.M., 2011. Multiscale processes leading to supercells in the landfalling outer rainbands of Hurricane Katrina. Wea. Forecast. 26, 828–847. https://doi.org/10.1175/WAF-D-10-05049.1, 2005.

Henderson, J., Nielsen, E.R., Herman, G.R., Schumacher, R.S., 2020. A hazard multiple: overlapping tornado and flash flood warnings in a National Weather Service forecast office in the southeastern United States. Wea. Forecasting 35, 1459–1481. https://doi.org/10.1175/WAF-D-19-0216.1.

Hill, E.L., Malkin, W., Schulz Jr., W.A., 1966. Tornadoes associated with cyclones of tropical origin - practical features. J. Appl. Meteorol. Climatol. 5, 745–763. https://doi.org/10.1175/1520-0450(1966)005<0745:TAWCOT>2.0.CO;2.

Huang, X.X., Yu, X.D., Yan, L.J., Li, Z.M., Li, C.L., 2018. Contrastive analysis of two intense typhoon-tornado cases with synoptic and Doppler weather radar data in Guangdong. J. Appl. Meteorol. Sci. 29, 70–83. https://doi.org/10.11898/1001-7313.20180107 (in Chinese with English abstract).

Kain, J.S., Weiss, S.J., Bright, D.R., Baldwin, M.E., Levit, J.J., Carbin, G.W., Schwartz, C.S., Weisman, M.L., Droegemeier, K.K., Weber, D.B., Thomas, K.W., 2008. Some practical considerations regarding horizontal resolution in the first generation of operational convection-allowing NWP. Wea. Forecast. 23, 931–952. https://doi.org/10.1175/WAF2007106.1.

Landsea, C.W., Franklin, J.L., 2013. Atlantic hurricane database uncertainty and presentation of a new database format. Mon. Wea. Rev. 141, 3576–3592. https://doi.org/10.1175/MWR-D-12-00254.1.

Li, Y., Chen, L., Zhang, S., 2004. Statistical characteristics of tropical cyclone making landfalls on China. J. Trop. Meteorol. 62, 541–549 (in Chinese with English abstract).

Malkin, W., Galway, J.G., 1953. Tornadoes associated with hurricanes. Mon. Wea. Rev. 81, 299–303. https://doi.org/10.1175/1520-0493(1953)081<0299:TAWH>2.0.CO;2.

Martinaitis, S., 2017. Radar observations of tornado-warned convection associated with tropical cyclones over Florida. Wea. Forecast. 32, 165–186. https://doi.org/10.1175/WAF-D-16-0105.1.

McCaul Jr., E.W., 1991. Buoyancy and shear characteristics of hurricane-tornado environments. Mon. Wea. Rev. 119, 1954–1978. https://doi.org/10.1175/1520-0493(1991)119<1954:BASCOH>2.0.CO;2.

McCaul Jr., E.W., Weisman, M.L., 1996. Simulations of shallow supercell storms in landfalling hurricane environments. Mon. Wea. Rev. 124, 408–429. https://doi.org/10.1175/1520-0493(1996)124<0408:SOSSSI>2.0.CO;2.

McCaul Jr., E.W., Buechler, D.E., Goodman, S.J., Cammarata, M., 2004. Doppler radar and lightning network observations of a severe outbreak of tropical cyclone tornadoes. Mon. Wea. Rev. 132, 1747–1763. https://doi.org/10.1175/1520-0493(2004)132<1747:DRALNO>2.0.CO;2.

McCaul Jr., E.W., Kirkpatrick, J.C., Cohen, C., 2018. A Parameter Space Approach to Understanding Convective Storm Morphology. Amer. Geophys. Union, Washington, DC, USA. https://doi.org/10.1002/essoar.10501513.1. Poster A11O-2487, Amer. Geophys. Union 2018 Fall Meeting.

McDonald, J.R., 2001. T. Theodore Fujita: his contribution to tornado knowledge through damage documentation and the Fujita scale. Bull. Amer. Meteorol. Soc. 82, 63–72. https://doi.org/10.1175/1520-0477(2001)000<0063:TTFHCT>2.3.CO;2.

Nowotarski, C.J., Spotts, J., Edwards, R., Overpeck, S., Woodall, G.R., 2021. Tornadoes in hurricane Harvey. Wea. Forecast. 36, 1589–1609. https://doi.org/10.1175/WAF-D-20-0196.1.

Orton, R., 1970. Tornadoes associated with hurricane Beulah on September 19-23, 1967. Mon. Wea. Rev. 98, 541–547. https://doi.org/10.1175/1520-0493(1970)098<0541:TAWHBO>2.3.CO;2.

Paredes, M., Schenkel, B.A., Edwards, R., Coniglio, M.C., 2021. Tropical cyclone outer size impacts the number and location of tornadoes. Geophys. Res. Lett. 48, e2021GL095922. https://doi.org/10.1029/2021GL095922.

Pearson, A.D., Sadowski, A.F., 1965. Hurricane-induced tornadoes and their distribution. Mon. Wea. Rev. 93, 461–464. https://doi.org/10.1175/1520-0493(1965)093<0461:HITATD>2.3.CO;2.

Rappaport, E.N., 2014. Fatalities in the United States from Atlantic tropical cyclones: new data and interpretation. Bull. Amer. Meteorol. Soc. 95, 341–346. https://doi.org/10.1175/BAMS-D-12-00074.1.

Ryzhkov, A.V., Schuur, T.J., Burgess, D.W., Zrnić, D.S., 2005. Polarimetric tornado detection. J. Appl. Meteorol. 44, 557–570. https://doi.org/10.1175/JAM2235.1.

Schaefer, J.T., Edwards, R., 1999. The SPC tornado/severe thunderstorm database. In: Preprints, 11th Conf. On Applied Climatology. Amer. Meteor. Soc., Dallas, TX, USA, pp. 215–220. https://www.spc.noaa.gov/publications/schaefer/database.htm.

Schenkel, B.A., Edwards, R., Coniglio, M.C., 2020. A climatological analysis of ambient deep-tropospheric vertical wind shear impacts upon tornadoes in tropical cyclones. Wea. Forecast. 30, 2033–2059. https://doi.org/10.1175/WAF-D-19-0220.1.

Schenkel, B.A., Coniglio, M.C., Edwards, R., 2021. How does the relationship between ambient deep-tropospheric vertical wind shear and tropical cyclone tornadoes change between coastal and inland environments? Wea. Forecast. 36, 539–566. https://doi.org/10.1175/WAF-D-20-0127.1.

Schneider, D., Sharp, S., 2007. Radar signatures of tropical cyclone tornadoes in central North Carolina. Wea. Forecast. 22, 278–286. https://doi.org/10.1175/WAF992.1.

Schultz, L.A., Cecil, D.J., 2009. Tropical cyclone tornadoes, 1950-2007. Mon. Wea. Rev. 137, 3471–3484. https://doi.org/10.1175/2009MWR2896.1.

Schultz, C.J., Peterson, W.A., Carey, L.D., 2011. Lightning and severe weather: a comparison between total and cloud-to-ground lightning trends. Wea. Forecast. 26, 744–755. https://doi.org/10.1175/WAF-D-10-05026.1.

Skamarock, W.C., Klemp, J.B., Dudhia, J., Gill, D.O., Barker, D.M., Duda, M.G., Huang, X.-Y., Wang, W., Powers, J.G., 2008. A description of the Advanced Research WRF version 3. NCAR Tech. 113. https://doi.org/10.5065/D68S4MVH. Note NCAR/TN-4751STR.

Smith, J.S., 1965. The hurricane-tornado. Mon. Wea. Rev. 93, 453–459. https://doi.org/10.1175/1520-0493(1965)093<0453:THT>2.3.CO;2.

Spratt, S.M., Sharp, D.W., Welsh, P., Sandrik, A.C., Alsheimer, F., Paxton, C., 1997. A WSR-88D assessment of tropical cyclone outer rainband

tornadoes. Wea. Forecast. 12, 479–501. https://doi.org/10.1175/1520-0434(1997)012<0479:AWAOTC>2.0.CO;2.

Sueki, K., Niino, H., 2016. Toward better assessment of tornado potential in typhoons: significance of considering entrainment effects for CAPE. Geophys. Res. Lett. 43, 12597–12604. https://doi.org/10.1002/2016GL070349.

Thompson, R.L., Vescio, M.D., 1998. The destruction potential index - a method for comparing tornado days. In: Preprints, 19th Conf. On Severe Local Storms. Amer. Meteor. Soc., Minneapolis, MN, USA, pp. 280–282. https://www.spc.noaa.gov/publications/thompson/dpi/dpi.htm.

Verbout, S.M., Schultz, D.M., Leslie, L.M., Brooks, H.E., Karoly, D.J., Elmore, K.L., 2007. Tornado outbreaks associated with landfalling hurricanes in the north Atlantic basin: 1954-2004. Meteorol. Atmos. Phys. 97, 255–271. https://doi.org/10.1007/s00703-006-0256-x.

Wind Science and Engineering Center, 2006. A Recommendation for an Enhanced Fujita Scale (EF-Scale), Revision 2. Texas Tech University Publication, p. 95. http://www.depts.ttu.edu/nwi/pubs/fscale/efscale.pdf.

Zhang, G.J., 2009. Effects of entrainment on convective available potential energy and closure assumptions in convective parameterization. J. Geophys. Res. 114, D07109. https://doi.org/10.1029/2008JD010976.